

Color restoration method of printing in machine visual detection

Peng Liu (刘 澎)^{1,2*}, Ning Zhao (赵 宁)¹, Linghui Ren (任玲辉)³, and Qianqian Xu (徐倩倩)²

¹Northwestern Polytechnical University, Xi'an 710072, China

²College of Printing and Packaging Engineering, Xi'an University of Technology, Xi'an 710048, China

³Xi'an Aerospace-huayang Printing & Packaging Machinery co., ltd, Xi'an 710100, China

*Corresponding author: lp11900@sohu.com

Received October 4, 2013; accepted October 16, 2013; posted online March 4, 2014

It is found that application of Retinex color constancy algorithm in machine vision can weaken light interference on printing chromatic aberration. We propose a new method of fusion of Weighted Least Squares and Multi-Scale Retinex in the $L^*a^*b^*$ color space for the purpose of further enhancing the degree of recovery of prints colors. The effectiveness of the proposed method is tested against experiments on images of the same original print acquired in different illuminants. The method exhibits a good application prospect in machine vision in virtue of its great color consistency capability in maintaining the color of the original print.

OCIS codes: 150.1135, 150.1708.

doi: 10.3788/COL201412.S11501.

The printed matters are widely used in the field of cultural communication, product packaging as well as securities. The print should be a life-like replication of the originals as far as possible, due to the special purpose. Since the printing speed can be as high as 18000 sheets per hour or 24000 meters per hour, a failure to detect printing errors in time will cause large amount of waste of paper and ink and will in consequence cause serious pollution problems. A news from MAIL ONLINE on 7th December 2010 reports that 'The \$100bn blunder: Fed forced to 'quarantine' one billion \$100 bills after printing error makes them worthless^[1]. A printing problem with the new high-tech \$100 bills has forced government printers to shut down production and to quarantine more than one billion of the notes. Therefore, printing defects can be timely detected, which is able to avoid the occurrence of major accidents if the printing machines are equipped with cutting-edge prints' detection system. As a result, fast and effective detection methods are worth of studying.

The images acquired by charge-coupled device (CCD) will vary along with the different colors of prints, which will not display the same color characteristics under different standard illuminants due to the unstable and uneven illuminants. As a result, the determination of colors will be influenced. In order to accurately detect the printing defects, it needs to enhance the defects information of printing image, and meanwhile, to weaken light interference on printing effectively, chromatic aberration is needed. Liu *et al.* proposed a method of color constancy enhancement under poor illumination. The method is to maintain the hue of an image during the processing so that the change of saturation can be minimized^[2]. Cheong^[3] proposed a method of color classification for color-based image code recognition, which is robust under varying environment conditions such as illuminants, cameras, and print materials. Funt *et al.*^[4,5]

proposed a method of color correction based on neural network. The model is limited to distinguish the coordinates of chromaticity image illumination, but failed to recognize the spectral energy distribution of the image illumination and therefore unable to obtain the surface reflection characteristics of the image. Chin *et al.*^[6] proposed a method based on histogram and neural network to estimate the power spectrum, with which the expressions of the spectral power distribution of the illuminant and object reflectance are simplified. The method has made big progress in solving the problem, of which color vision is not fully constrained. With this method, high precision of color correction can be obtained, but the spectral power distribution is difficult to obtain.

Starting from the perceptual characteristics of the object color of human eyes, Retinex will be applied to the reproduction of printing color in this article. The following improvements have been made to supply the deficiencies of Retinex. First, in order to keep a color information, we convert RGB color model images into $L^*a^*b^*$ color model images. In L^* channel, we use Retinex method to remove the light effect, with which the effect on chromatic aberration from uneven illuminant can be effectively reduced, so that the color constancy of the acquired print colors can be obtained under uneven light within a certain scope. Second, we use weighted least square (WLS) filtering to enhance the defect information of printing image for detection.

The perception of object color of human eyes remains relatively constant while illumination conditions change, which shows the color constancy of human eyes. The Retinex model for the computation of lightness was introduced by Land and McCann^[7]. Retinex calculations aim to calculate the sensory response of lightness. It is important to distinguish three entities, physical reflectance, the sensation of lightness, and perceived reflectance, from each other. Colors of the objects have little

relationship to the lighting environment; it is only determined by the surface relation properties of the visual system. In our method, the radiation image is estimated from the original image, and then it is subtracted from the original image to get the reflection image of the nature of the object. Lighting component that is relevant to the illuminant is determined by the lighting source. That is

$$I(x, y) = R(x, y) \bullet L(x, y), \quad (1)$$

where $L(x, y)$ indicates the incident sunlight, which is the brightness component, and it is the low-frequency information changing slowly; $R(x, y)$ indicates the reflection properties and has nothing to do with the light; $I(x, y)$ is the reflected light, the same image as what we achieved. The reflection component $R(x, y)$ is determined by the material and shape of the object. It can also be understood as high-frequency information; $L(x, y)$ is low-frequency information. Retinex algorithm can get reflection properties from the image $I(x, y)$ in all the manner of mathematical ways without considering the L , the incident component. Since $R(x, y)$ and $L(x, y)$ are unknown, Eq. (1) is an indefinite equation to get reflection component and brightness component from the given image $I(x, y)$. It fits better the perception of human vision if Eq. (1) is written in the Logarithm scale as

$$R = \log(I(x, y)) - \log(L(x, y)), \quad (2)$$

where L is the estimated lightness component by the illuminant estimation algorithm; R is the output image of $R(x, y)$ after the addition and subtraction operations. Retinex is divided into single-scale Retinex algorithm and multi-scale Retinex algorithm.

A single-scale model can attempt to calculate only one of the three goals of the Retinex algorithm, which is to calculate the sensation of lightness. Considering the case of two faces of a white cube, one in the direct sunlight and the other in the shadow, the physical reflectance is a measure of a property of the cube's surface relating its radiance to its irradiance. The calculation formula of the single-scale Retinex is shown as

$$\begin{cases} \bar{R}(x, y) = \log(I(x, y)) - \log(G(x, y) * I(x, y)) \\ G(x, y) = K \exp\left(-\frac{x^2 + y^2}{\sigma^2}\right) \\ \iint G(x, y) dx dy = 1. \end{cases} \quad (3)$$

In Eq. (3), $\bar{R}(x, y)$ is the estimated term of $R(x, y)$ in log-domain, K is the normalization coefficient calculated with $\iint G(x, y) dx dy = 1$, and σ means the scale of the Gaussian filter. The smaller σ is, the better the details of the darker regions can be enhanced and then producing color distortion. On the contrary, the greater σ is, the higher fidelity of color is kept, while compression capacity of dynamic range diminished.

Multi-Scale Retinex (MSR) is a new synthesis of the single-scale Retinex (SSR) algorithm. It could obtain the result by calculating weighted sums of different scales of single scale Retinex, so it has Local and

Global dynamic range and color constancy and its formula is as

$$R_i(x, y) = \sum_{k=1}^K W_k (\log I_i(x, y) - \log(F_k(x, y) \times L_i(x, y))), \quad (4)$$

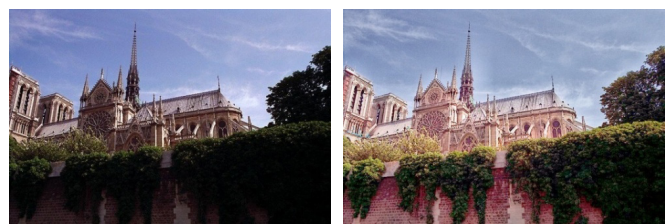
where $R_i(x, y)$ is the output value of the i th channel and $I_i(x, y)$ is the pixel value, $F_k(x, y)$ indicates the around function and K is the number of the around functions and W_k is the weight, $\sum_{k=1}^K W_k = 1$.

Fig. 1 is a Retinex processing result of image affected by light sources, and it can be seen that the multi-scale Retinex showed a better effect.

Retinex tone-mapping can produce the phenomenon of 'halation' because of the flatness of Gaussian filter when evaluating the lighting component. The lighting component that we got in this way could not preserve important edge information generated by illumination change. The lighting component we get from the image after smoothing process cannot retain the trends of gradient distribution of the edge of original image, so this results in the phenomenon of 'halation'.

For this reason, we prefer to use the filter that is based on WLS, raised by Zeev Farbman in 2008^[8]. By using the idea of approximation, WLS can get the lighting component by solving the elliptical part differential equation with an iterative approach. The lighting component could keep the essential features and flatness simultaneously, meaning that it could preserve important edge information generated by illumination change and make the image smoothing so that there is no halation.

The RGB channel results could influence each other, so we prefer the $L^*a^*b^*$ color space, we balance and recover the luminance of the luminance channel and then combine with a^* and b^* channel to recover the color. Because of having no disposal of the color channels, the color relation of pixel does not change, leading to the effect of removing light and keeping color of the image; The smaller the σ is, the better processing effect of the details in dark regions, but smaller contrast



(a) Effected by illuminant

(b) SSR result

(c) MSR result

Fig. 1. Retinex.

range and color distortion; otherwise the color fidelity will be improved, but having less control over the ability of compressing the dynamic range. Multi-scale could produce a better color and dynamic range but halation, so we prefer a new filter to take the place of Gaussian filter.

CIE $L^*a^*b^*$ is the most complete color space specified by the International Commission on Illumination. This color model is determined by neither the light nor the pigment. It is a uniform color space that reflects the way human observes color and it is in favor of image processing. It describes all the colors visible to the human eyes and was created to serve as a device-independent model to be used as a reference. The three coordinates of CIE $L^*a^*b^*$ represent the lightness of the color ($L^* = 0$ yields black and $L^* = 100$ indicates diffuse white), its position between red/magenta and green (a^* , negative values indicate green while positive values indicate magenta) and its position between yellow and blue (b^* , negative values indicate blue and positive values indicate yellow).

Since the $L^*a^*b^*$ model is a three-dimensional model, it can only be represented properly in a three-dimensional (3D) space. Two-dimensional (2D) depictions include chromaticity diagrams: sections of the color solid with a fixed lightness. It is crucial to realize that the visual representations of the full gamut of colors in this model are never accurate; they are there just to help in understanding the concept.

Because the red-green and yellow-blue opponent channels are computed as differences of lightness transformations of (putative) cone responses, CIELAB is a chromatic value color space. The nonlinear transformed equation from RGB to $L^*a^*b^*$ color space is shown as

$$\begin{bmatrix} X \\ Y \\ Z \end{bmatrix} = \begin{bmatrix} 0.607 & 0.174 & 0.200 \\ 0.299 & 0.587 & 0.144 \\ 0.000 & 0.066 & 1.116 \end{bmatrix} \begin{bmatrix} R \\ G \\ B \end{bmatrix}, \quad (5)$$

$$\begin{cases} L^* = 116(Y/Y_0)^{1/3} - 16 & (Y/Y_0) > 0.01 \\ a^* = 500[(X/X_0)^{1/3} - (Y/Y_0)^{1/3}] \\ b^* = 200[(Y/Y_0)^{1/3} - (Z/Z_0)^{1/3}] \end{cases}, \quad (6)$$

where X , Y , Z are tristimulus values of the color sample; X_0 , Y_0 , Z_0 are tristimulus values of CIE standard illuminant; L^* is psychometric brightness, a^* , b^* are psychometric chromaticity, the same as red-green and yellow-blue reflections of gangliocyte.

The Color difference formula is

$$\Delta E_{lab}^* = \sqrt{(L_1^* - L_2^*)^2 + (a_1^* - a_2^*)^2 + (b_1^* - b_2^*)^2}. \quad (7)$$

Hue and color predictors are like these:

$$h_{ab} = \tan^{-1}(b^*/a^*), \quad (8)$$

$$C_{ab}^* = \sqrt{(a^*)^2 + (b^*)^2}. \quad (9)$$

In Fig. 2, Zeev Farberman^[8] showed us the processing results using Gauss filter and WLS filter. We can find edge blur when using Gauss filter. WLS filter eliminates image noise while it retains edge details successfully.

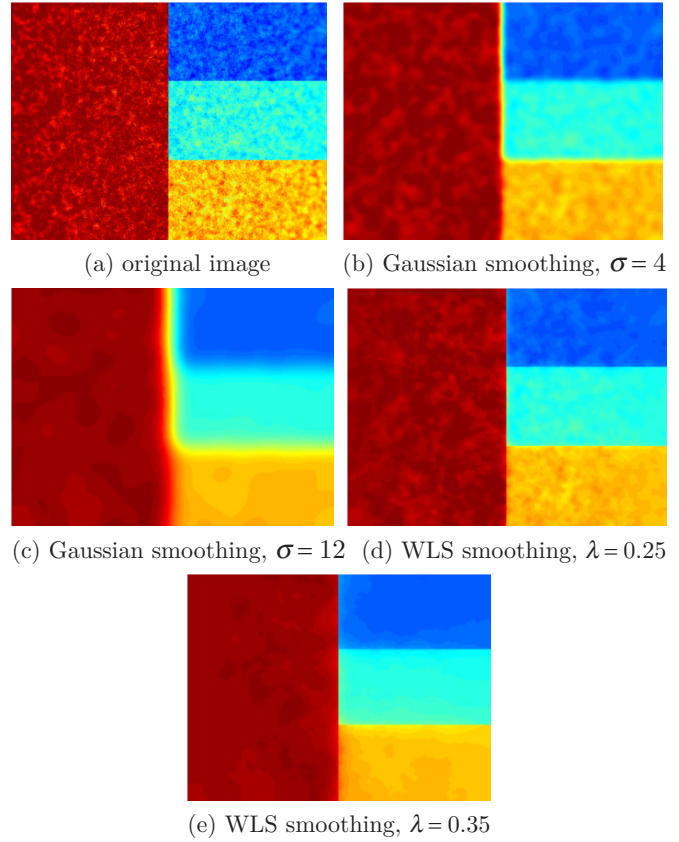


Fig. 2. WLS filter contrast with the Gaussian filter.

The essence of WLS filter is, given an input image g , to get a new image u . The new image u is required to be as close as possible to the input image g . On the other hand, it should be as smooth as possible. u should keep the flatness and retain basic properties of g , simultaneously. This problem turns into the salvation of image u to minimize the value of quadratic target function^[8] as follows:

$$E = \sum_p ((u_p - g_p)^2 + \lambda \left(a_{x,p}(g) \left(\frac{\partial u}{\partial x} \right)^2 + a_{y,p}(g) \left(\frac{\partial u}{\partial y} \right)^2 \right)), \quad (10)$$

in which the index p is the spatial position of a pixel. In the formula, $(u_p - g_p)^2$ is the least square error, which is used to keep u and g to be as similar as possible. The second item is smooth condition, which is used to retain the smoothness of image u by minimizing partial differential functions $\frac{\partial u}{\partial x}$, $\frac{\partial u}{\partial y}$. $a_{x,p}(g)$ and $a_{y,p}(g)$ are smoothing weights, which are determined by the image g . That is

$$\begin{cases} a_{x,p}(g) = \left(\left| \frac{\partial l}{\partial x}(p) \right|^\alpha + \epsilon \right)^{-1} \\ a_{y,p}(g) = \left(\left| \frac{\partial l}{\partial y}(p) \right|^\alpha + \epsilon \right)^{-1} \end{cases}, \quad (11)$$

where the parameter α is used to control the level of sensitivity of edging in the smoothing process. Generally, it is between 1.0 and 1.8. The parameter ϵ is chosen

as 0.00001 to prevent the denominator being zero. The parameter λ is to adjust the relative weight relation between smooth condition and the least square error. We could get different images with different smoothness by changing the value of λ , so λ can be regarded as a scale parameter. Eq. (10) could be expressed in the matrix form as

$$E = (u - g)^T (u - g) + \lambda (u^T D_x^T A_x D_x u + u^T D_y^T A_y D_y u). \quad (12)$$

In this formula, A_x and A_y are diagonal matrices, the diagonal elements are smoothing weights $a_{x,p}(g)$ and $a_{y,p}(g)$; D_x and D_y are discrete differential operators. Taking the derivative of u and making it zero, we will get the formula as

$$\frac{\partial E}{\partial u} = 2(u - g) + 2\lambda (D_x^T A_x D_x + D_y^T A_y D_y)u = 0. \quad (13)$$

The simplification of the formula above is

$$(I + \lambda (D_x^T A_x D_x + D_y^T A_y D_y))u = g, \quad (14)$$

where I is an unit matrix. Then we define

$$L_g = D_x^T A_x D_x + D_y^T A_y D_y. \quad (15)$$

So, the image u is determined by this linear equation:

$$(I + \lambda L_g)u = g. \quad (16)$$

This equation has solutions while the coefficient matrix is nonsingular:

$$u = (I + \lambda L_g)^{-1} g. \quad (17)$$

We can find the solutions of this algebraic equation by using the Conjugate Gradient (CG) method^[9].

Knowing from the equation λ is the scale parameter of WLS filter. Thus, we can get results as follows by using Eq. (10):

$$L_1(x, y) = (I + \lambda_1 L_g)^{-1} \log I(x, y), \quad (18)$$

$$L_2(x, y) = (I + \lambda_2 L_g)^{-1} \log I(x, y), \quad (19)$$

$$L_3(x, y) = (I + \lambda_3 L_g)^{-1} \log I(x, y), \quad (20)$$

where I is the unit matrix and $\log I(x, y)$ is the brightness value of the point (x, y) in the Log-domain, $\lambda_1, \lambda_2, \lambda_3$ are three different scale-parameters and $L_1(x, y)$, $L_2(x, y)$, and $L_3(x, y)$ are illuminated images with different scales.

We replace the filter in multi-scale Retinex with WLS filter, as in

$$R(x, y) = \sum_{k=1}^K W_k (\log I(x, y) - \varphi_k \times L_k(x, y)). \quad (21)$$

φ_k 's value can be taken in the region of $[0.0, 1.0]$. We can use different values for different scales. K is the number of scales.

First, we take the index of $R(x, y)$:

$$R'(x, y) = \exp(R(x, y)). \quad (22)$$

Secondly, we normalize the equation above:

$$R''(x, y) = \frac{R'(x, y) - \min(R'(x, y))}{\max(R'(x, y)) - \min(R'(x, y))}. \quad (23)$$

Finally, we regulate the image brightness by using Drago's self-adapting function^[10] and then turn it into the gray level of $[0, 255]$. That is

$$I_{out} = (R''(x, y))^{\frac{\log(b)}{\log(0.5)}} \times 255, \quad (24)$$

where b is the controllable parameter from 0.5 to 1.0. We can get images in different grayscales by changing the parameter b .

We decide to use the schlock's method for color restoration^[9]. This method uses S to be sure we are in control of saturation. The formula is as

$$R_{out} = \left(\frac{R}{I}\right)^s * I_{out}, \quad (25)$$

$$G_{out} = \left(\frac{G}{I}\right)^s * I_{out}, \quad (26)$$

$$B_{out} = \left(\frac{B}{I}\right)^s * I_{out}, \quad (27)$$

where I is the brightness value of input image, I_{out} is the processed brightness value.

Blocks of color tables have been made containing yellow color bar, color bar magenta and cyan color bar in order to verify the proposed method. There are eleven color blocks for each color. Among all the color bars, each color bar is composed of small patches, of which the dot area ratio is 30%–80%. The region is more sensitive to the change of illumination.

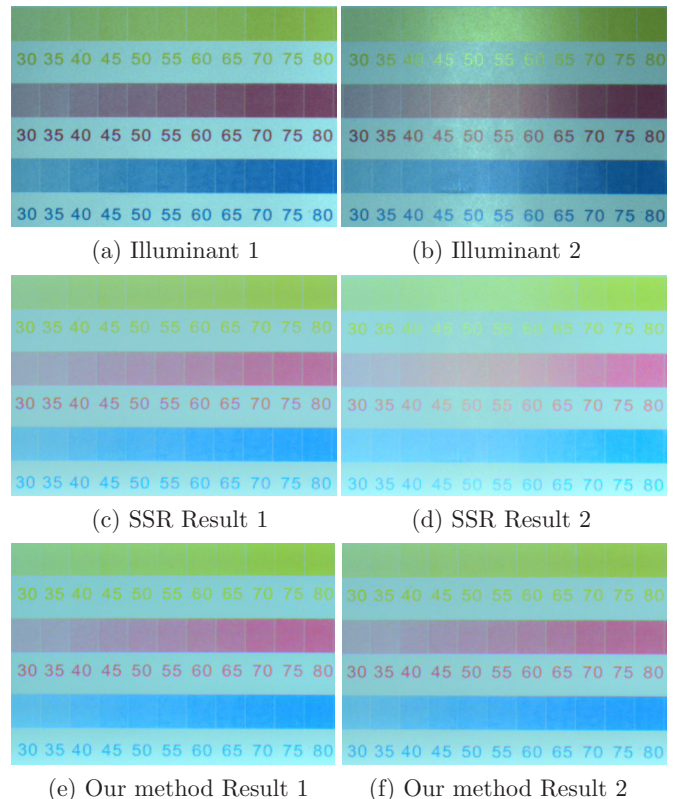


Fig. 3. Comparison of results.

Images of the same original print acquired under different illuminants can be seen in Fig. 3(a) and (b), in which different color characteristics are shown before being processed. The images processed by SSR method exhibit consistency of color, indicating SSR method provides effective performance in color constancy—refer Fig. 3(c) and Fig. 3(d). The color of images processed by the method $L^*a^*b^*$ -WLS-MSR proposed in this article provide more uniformity in color change, such as shown in Fig. 3(e) and Fig. 3(f).

Images in Fig. 4 are selected from the first and the last row of Fig. 3, corresponding to Fig. 3(a), Fig. 3(b), Fig. 3(e), and Fig. 3(f). We select 50% dot area of magenta color lump to observe the color values. In Fig. 4(a) and Fig. 4(b), values are different in RGB coordinate. On the contrary, in Fig. 4(c) and Fig. 4(d), values are almost same. It shows a good color consistency in the $L^*a^*b^*$ color space, indicating that the proposed method can reproduce color to a certain extent.

Generally, we use Formula (28) to contrast this color to another in RGB scale:

$$\Delta E_{rgb} = \sqrt{(R_1 - R_2)^2 + (G_1 - G_2)^2 + (B_1 - B_2)^2}. \quad (28)$$

In Fig. 5, the vertical coordinates of C, M, and Y represent the color difference between Fig. 3(a) and Fig. 3(b) in RGB color space, while the horizontal coordinates represent 11 color lumps of the C, M, and Y. The images are acquired from the same print under different lighting conditions, of which the color difference of each

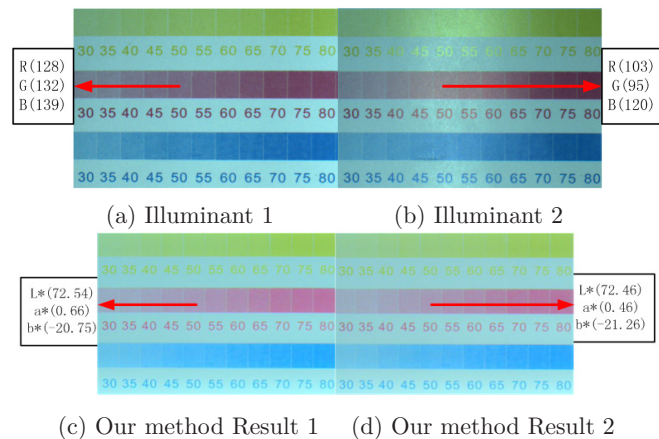


Fig. 4 Numerical comparison before and after processing.

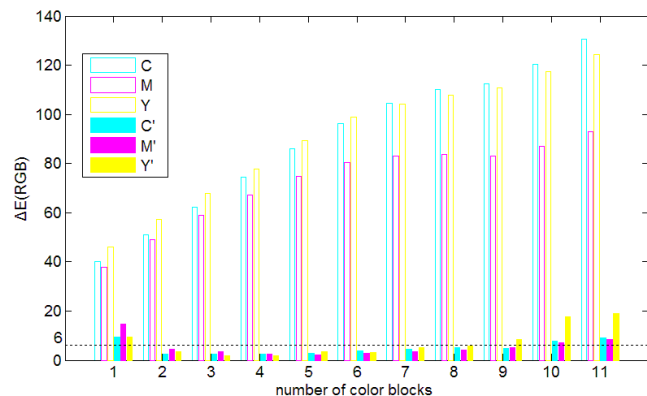


Fig. 5. RGB Color difference pre-and post-SSR processing.

is more than 35, which is calculated with Eq. (28). The vertical coordinates of C',M',Y' represent the color difference between Fig. 3(c) and Fig. 3(d) in the RGB color space, while the horizontal coordinates represent 11 color lumps. Fig. 3(c) and Fig. 3(d) are processed by the SSR algorithm after being acquired under different lighting conditions. By computing the color difference between Fig. 3 (c) and Fig. 3 (d) with Eq. (28), the result is about 6, which is the threshold value of a noticeable difference.

In Fig. 6, the vertical coordinates of C, M, Y represent the color difference between Fig. 3(a) and Fig. 3(b) in $L^*a^*b^*$ color space, of which the color difference of each is more than 22, which is calculated with Formula (7). The vertical ordinates of C', M', Y' represent the color difference between Fig. 3(e) and Fig. 3(f) in the $L^*a^*b^*$ color space. Fig. 3(e) and Fig. 3(f) are processed by our method and the color difference between Fig. 3(e) and Fig. 3(f) is less than 6.

As a result, our $L^*a^*b^*$ -WLS-Retinex algorithm performs excellently in maintaining color consistency, weakening the interference of illumination. The prints after the process can offer a strong basis for the subsequent printing defects judgment.

To evaluate the outcome of enhancement, we use information entropy to evaluate how much details of the image. We compute information entropy separately in Table 1 and the values are 7.3498, 7.6730, and 7.7283. These values indicate that our process enhances the information of details effectively.

The color constancy theory proposed by Land was found have great potential to remove the light interference with in-depth analysis of the color vision theory, according to the characteristics of the printed image and color vision theory. In this paper, Retinex theory has been introduced to print machine vision detection areas as a method of image pre-process to resolve the interference of illumination on the color difference.

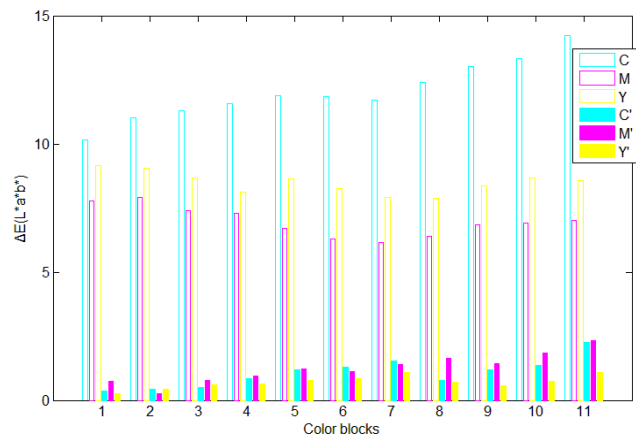


Fig. 6. $L^*a^*b^*$ Color difference pre-and post-our method processing.

Table 1. Information Entropy

Parameter	SSR	MSR	Our method
Entropy	7.3498	7.6730	7.7283

At the same time, $L^*a^*b^*$ -WLS-Retinex method is proposed.

The experiments show that:

(1) The application of Retinex in printing machine vision process performed great color retention. This method can be utilized to eliminate the interference of uneven illumination on the printed image to some extent.

(2) The Retinex methods of the $L^*a^*b^*$ color space are more conducive to maintain print color than that of RGB color space.

(3) This paper presents an improved WLS-Retinex algorithm in the $L^*a^*b^*$ color space, which can enhance the defects information to be used as pre-processing algorithm of images in detecting print defect, providing a basis for the subsequent prints defects judgment.

This work was supported by the National Natural Science Foundation of China (Grant No. 51275406) and the National Science and Technology Support Program of China (Grant No. 2013BAF04B01).

References

1. DAILY MAIL reporter, <http://www.dailymail.co.uk/news/article-1336287/Fed-forced-quarantine-1b-100-bills-printing-error-makes-worthless.html> (December 7, 2010).
2. L. Jun, S. Zhenfeng, and C. Qimin, *Optics Letters* **24**, 4821 (2011).
3. Cheong C, Bowman G, Han TD, *Applied Optics* **13**, 2326 (2008).
4. B. V. Funt, V. C. Cardei, and K. Bamard, "Method of estimating chromaticity of illumination using neural networks," U.S. patent 5,907,629, (1999).
5. V. C. Cardei, B. V. Funt, and K. Bamrad, *Journal of the optical Society of America*, **19**, 2374 (2002).
6. C. Tenglin, Wefan, and Changeheng, *IEEE International Conference on Systems, Man and Cybernetics*, 2488 (2005).
7. E. H. Land and J. J. McCann, *Journal of the Optical Society of America*, **61**, 1 (1971).
8. Z. Farbman, R. Fattal, D. Lischinski, and R. Szeliski, *Proceedings of ACM SIGGRAPH, California*, 1 (2008).
9. JR. Shewchuk. Technical Report, CMU-CS-94-125, Pittsburgh, School of Computer Science, Carnegie Mellon University, 1994: 30.
10. F. Drago, K. Myszkowski, T. Annen, *Computer Graphics Forum* **22**, 419 (2003).